

Dalton Transactions

Synthesis of Organo-uranium(II) Species in the Gas-phase using Reactions Between [UH]+ and Nitriles

Journal:	Dalton Transactions
Manuscript ID	DT-ART-09-2024-002508.R2
Article Type:	Paper
Date Submitted by the Author:	31-Oct-2024
Complete List of Authors:	Terhorst, Justin; Duquesne University Bayer School of Natural and Environmental Sciences Corcovilos, Theodore A.; Duquesne University, Physics Lenze, Samuel; Duquesne University Bayer School of Natural and Environmental Sciences, Department of Chemistry and Biochemistry van Stipdonk, Michael; Duquesne University, Chemistry and Biochemistry

SCHOLARONE™ Manuscripts

ARTICLE

Synthesis of Organo-uranium(II) Species in the Gas-phase using Reactions Between [UH]⁺ and Nitriles

Received 00th January 20xx, Accepted 00th January 20xx

DOI: 10.1039/x0xx000000x

Justin G. Terhorst, a Theodore A. Corcovilos, b Samuel, J. Lenze, a and Michael J. van Stipdonka

One challenge in the quest to map the intrinsic reactivity of model actinide species has been the controlled synthesis of organo-actinide ions in the gas phase. We report here evidence that a series of gas-phase, σ -bonded [U-R]⁺ species (where R = CH₃, C₂H₃, C₂H₅, C₃H₇, or C₅H₆) can be generated for subsequent study of ion-molecule chemistry by using preparative tandem mass spectrometry (PTMSⁿ) via ion-molecule reactions between [UH]⁺ and a series of nitriles. Density functional theory calculations support the hypothesis that the [U-R]⁺ ions are created in a pathway that involves intramolecular hydride attack and the elimination of neutral HCN. Subsequent reactivity experiments revealed that the [UCH₃]⁺ readily undergoes hydrolysis, yielding cationic uranium hydroxide ([UOH]⁺) and methane (CH₄). Other possible reaction pathways, such as the spontaneous rearrangement to [HU=CH₂]⁺, are shown by theoretical calculations to have energy barriers, strengthening the evidence for the formation of a σ -bonded [U-CH₃]⁺ complex in the gas-phase.

Introduction

Homoleptic σ -bonded uranium-alkyl complexes have been a synthetic goal since the time of the Manhattan Project.¹ One motivation for initial investigations was potential use of organoactinide complexes for isotope enrichment.¹⁻³ Current interest in these species stems from their potential use in catalytic processes and as an opportunity to investigate the fundamental f-orbital involvement in the making and breaking of bonds.⁴ In general, uranium-alkyls are attractive candidates for new catalytic applications such as hydrogenation, hydroformylation, alkene isomerization, and olefin polymerization.^{1,4} They also offer large ionic radii, which can allow coordination of large ligands, and provide access to higher coordination numbers compared to d-block elements.

The significant role of σ -bonded transition metal organometallic species in organic synthesis, along with their unique structures and reactivity, makes the generation of analogous uranium-alkyls a compelling goal. The first thermally stable, σ -bonded uranium-alkyl complexes were synthesized and characterized by Marks , and, later, Wilkinson and Sigurdson isolated a series of homoleptic uranium-alkyls. In general, homoleptic U-alkyls are more difficult to isolate than complexes supported by ancillary ligands due to their thermal instability, making them quite rare. The synthesis of organouranium complexes typically involves U-centers supported by pentamethylcyclopentadienyl (Cp*) , cyclopentadienyl (Cp), tris(3,5-dimethyl-1-pyrazolyl)borate (Tp*), ferrocene, alkoxide,

on the oxidation states of III, IV, and VI. 1 Theoretical studies of the U–C alkyl σ -bond indicate that the interaction has a significant amount of covalent character with notable contributions from the 6d and potentially the 5f orbitals. 26,27 We note that the involvement of the 6d and 5f orbitals in actinide bonding remains a topic of considerable discussion. $^{26-37}$ A major advance towards generating U-alkyls in the gas

and or oxo ligands to provide stability, and is primarily focused

A major advance towards generating U-alkyls in the gas phase has been the design of approaches to activate and eliminate the thermally stable (axial) oxo ligands from the uranyl (UO₂²⁺) moiety.³⁸⁻⁴⁷ Most important to the current study, we have shown that the oxo-uranium methylidyne intermediate, [OUCH]⁺, generated by collision-induced dissociation (CID) of a UO₂²⁺ precursor, can be used as a platform to create and study reactive organo-uranium species unfettered by the influences of the condensed phase such as solvent or counter ions. We note that gas-phase experiments are attractive because very small amounts of material (e.g. 10⁻⁴ grams or less) are needed for the mass spectrometry experiments, in addition to the inherent safety afforded by carrying the experiments out in the confines of an ion-trap mass spectrometer.

A recent study by our group has shown that the uranium hydride cation, $[UH]^+$, can be generated by CID of $[OUCH]^{+,47}$ This led us to consider whether gas-phase reactions between $[UH]^+$ and neutral nitriles (R-CN) could be used to create a series of σ -bonded $[U-R]^+$ ions. The results communicated here strongly suggest that a series of gas-phase, unsupported, formally organo-uranium(II) species, $[U-R]^+$, where $R=CH_3$, C_2H_3 , C_2H_5 , C_3H_7 , or C_5H_6 , can be generated in the gas phase for subsequent study of ion-molecule chemistry. Our experimental observations are supported by density functional theory (DFT) calculations which suggest: (a) a feasible common mechanism by which $[U-R]^+$ is formed by reaction between $[UH]^+$ and

^oDepartment of Chemistry and Biochemistry, Duquesne University, Pittsburgh, PA 15282, USA. E-mail: vanstipdonkm@duq.edu

^bDepartment of Physics, Duquesne University, Pittsburgh, PA 15282, USA

[†] Supplementary Information available (Additional computational information). See DOI: 10.1039/x0xx00000x

nitriles, and (b) rearrangement to a more stable formal oxidation state (i.e. U^{VI}) isomer is unlikely. In addition, the subsequent reactivity of $[U-R]^+$ with H_2O was probed, and the observed spontaneous hydrolysis supported by DFT calculations.

Results and Discussion

Preparative tandem mass spectrometry (PTMSⁿ) experiments were performed on a commercially available electrospray ionization (ESI), linear ion trap mass spectrometer that has been modified to allow the introduction of neutral reagents into the ion trap through the helium buffer gas line for the study of ion-molecule reactions. Details about the instrument are provided in the SI. Each experiment described below begins with production of the [UH]⁺ ion (m/z 239) by PTMSⁿ. The conversion of a UO₂²⁺ precursor ion to [UH]⁺ by removal of both "yl" oxo ligands is discussed in detail elsewhere and in the SI.⁴⁷ Briefly, creation of [UH]⁺ begins with CID of a solvent-coordinated (generally H₂O or CH₃OH) uranyl propiolate cation ([UO₂(O₂C-C=CH)]⁺) to furnish [OUCH]⁺, which is a reactive intermediate that has been studied by our group. A subsequent CID step is used to generate [UH]⁺ from [OUCH]⁺ by elimination of CO.

It is important to note that once [UH]+ has been generated and is isolated, reactions with background gasses such as O2 and H₂O present in the vacuum system of the ESI mass spectrometer (mass spectra shown in the SI) can produce $[U(OH)]^+$ (m/z 255) by hydrolysis, $[OUH]^+$ (m/z 255) or $[UO]^+$ (m/z 254) via reactions with O₂, and subsequent reactions with these ions products can generate [UO₂]+ (m/z 270), [UO(OH)]+, and $[UO_2H]^+$ (m/z 271). As a control, background spectra were collected by isolation of [UH]+ in the ion trap instrument without the deliberate addition of a neutral reagent. In addition to this, the reactivity specific to the hydride reagent ions was confirmed by comparison to the isolation of U^+ (m/z 238) which is created using the CID of [UH]*. In this case, U* was allowed to react with the background atmosphere gases and intentionally added neutral reagents under identical experimental conditions. It was found from the reactions of O₂ and H₂O with U⁺ produced $[UO]^+$ (m/z 254) and $[U(OH)]^+$ (m/z 255) respectively, in addition to $[UO_2]^+$ (m/z 270) and $[UO(OH)]^+$ (m/z 271) through an additional equivalent of O2. This illustrated the difference in reactivity of the two ions with or without the hydride ligand, to demonstrate that formation of [U-R]+ requires the [UH]+ "reagent" ion.

Reaction of [UH]+ with Acetonitrile and Propionitrile

The first experiment performed involved the reaction between [UH]⁺ and acetonitrile (CH₃CN). As described above, the hypothesis tested was that creation of [U-CH₃]⁺ would occur by loss of hydrogen cyanide neutral (HCN) in a metathesis reaction. The product ion spectra generated by isolation of [UH]⁺ or U⁺ and exposure to neutral CH₃CN are provided in Figure 1a and 1b, respectively at 100ms isolation time. The results of subsequent reactivity experiments using [U-CH₃]⁺ to confirm its composition through hydrolysis and CID are shown in Figures 1c

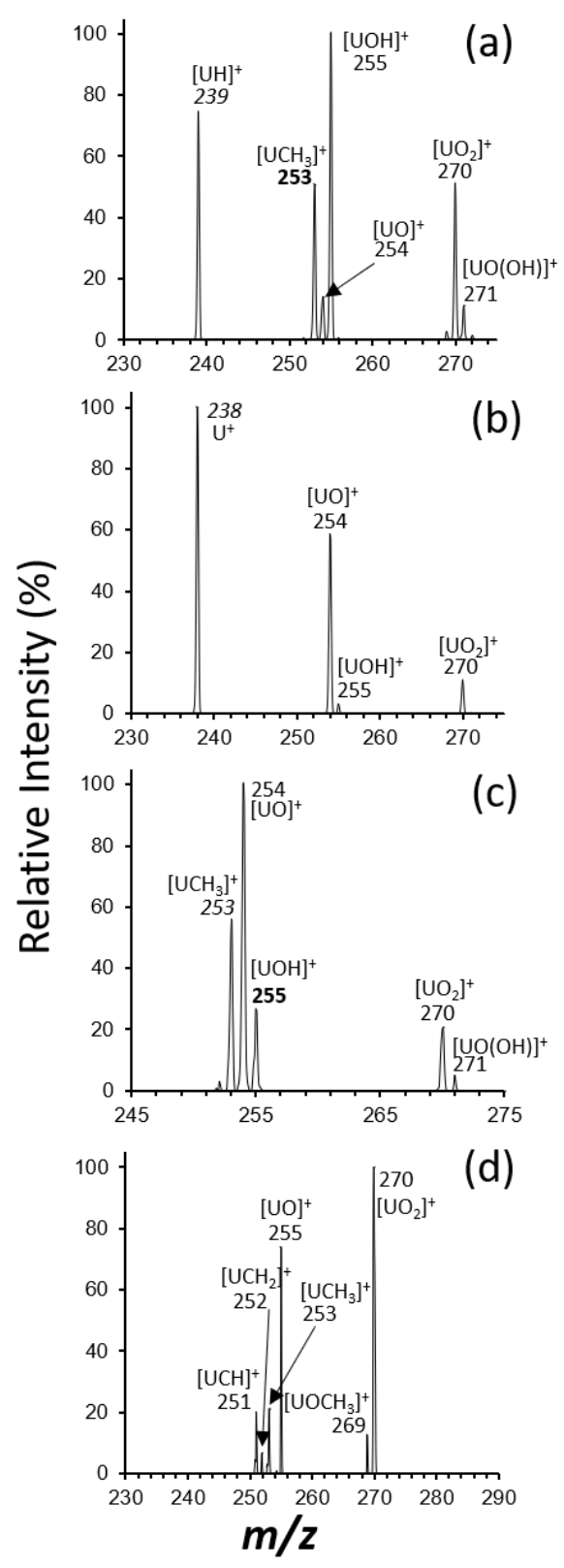


Figure 1: (a) Isolation of m/z 239 ([UH]+) at 100ms with deliberate introduction of CH₃CN. (b) Isolation of m/z 238 (U⁺) at 100ms to react with CH₃CN. (c) Isolation of m/z 253 ([UCH₃]⁺) at 100ms to react with background O₂ and H₂O. (d) CID of m/z 253 ([UCH₃]⁺) at 10% normalized collision energy; activation Q =0.30.

Journal Name ARTICLE

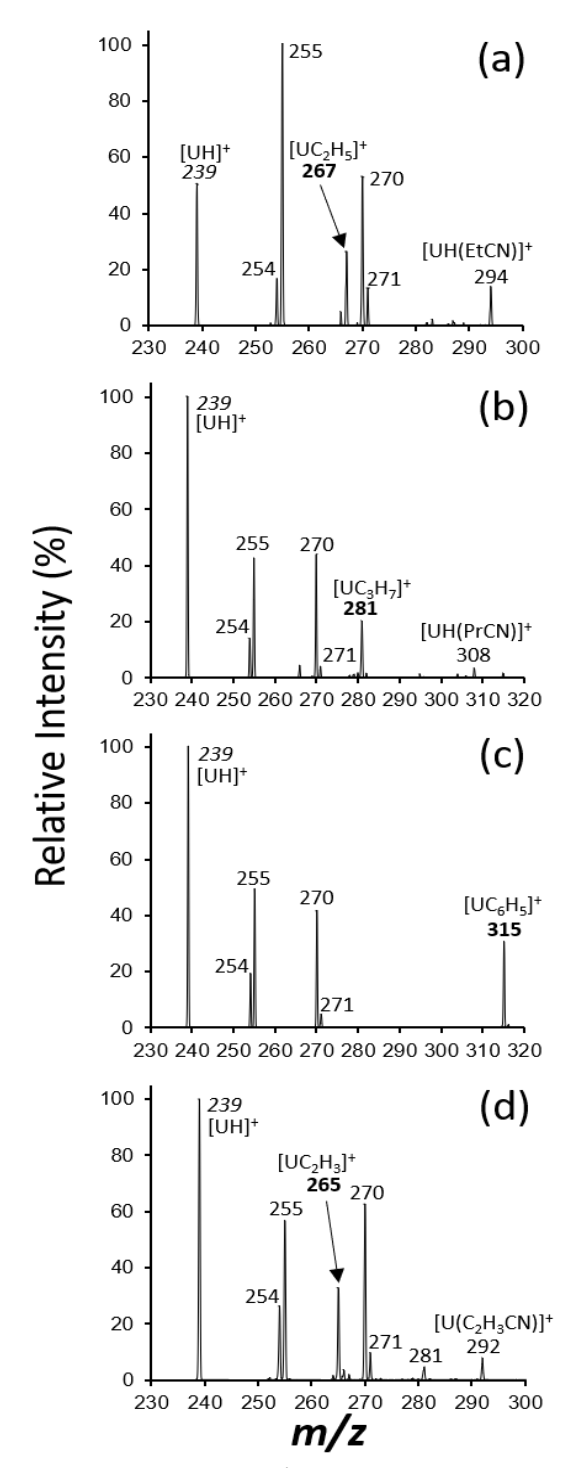


Figure 2: (a) Isolation of m/z 239 ([UH]*) with deliberately introduced CH₃CH₂CN at 100ms. (b) Isolation of m/z 239 ([UH]*) with deliberately introduced CH₃CH₂CN at 100ms. (c) Isolation of m/z 239 ([UH]*) with deliberately introduced C₆H₅CN at 100ms. (d) Isolation of m/z 239 ([UH]*) with deliberately introduced CH₂CHCN at 100ms.

and 1d, respectively. For isolation of $[UH]^+$ at m/z 239, comparison with the spectra collected with or without the presence of CH_3CN clearly identified a product ion at m/z 253, which is consistent with the creation of $[UCH_3]^+$ by reaction 1.

As shown in Figure 1b, the peak at m/z 253 was not observed following isolation of U⁺ at m/z 238 under similar experimental conditions.

$$[UH]^{+} + CH_{3}CN \rightarrow [U-CH_{3}]^{+} + HCN \qquad (1)$$

To confirm the assignment of composition of the peak at m/z 253 as [UCH₃]⁺, rather than, for example, [UNH]⁺, identical experiments were performed using CD₃CN. With the labeled neutral reagent, a shift of 3 m/z units was observed, consistent with the addition of 3 H atoms by reaction 1 (spectra not shown).

It should be noted that the neutral hydrogen cyanide product is not observed in the mass spectrometry experiments, but the elimination is inferred by conservation of mass. We note that the proposed reaction pathways are supported by density functional theory (DFT) calculations described below. Moreover, to distinguish different structural isomers and possible rearrangements, DFT was employed to determine the energetic barriers. It should also be emphasized that the reactions that are observed in the mass spectrometer are carried out at a roughly ambient effective temperature, without any deliberate heating after isolation. Therefore, the apparent formation of [U-CH₃] by reaction of [UH] with CH₃CN is spontaneous.

Subsequent CID of [U-CH₃]⁺ (m/z 253, Figure 1c) using relatively mild collisional activation (experimental details are provided in the SI) generated peaks at m/z 252 and m/z 251.We attribute the former to the loss of H., possibly by rearrangement of [U-CH₃]⁺ to [HU=CH₂]⁺ followed by homolytic cleavage of the hydride. Creation of the latter product ion appears to involve dehydrogenation to eliminate H2. Note that in this experiment the need for collisional activation demonstrates that the loss of H• or H2 are endothermic processes, consistent with previous computational and experimental work that probed collisions between U+ and CH₄.^{48,49} The rearrangement process for [U-CH₃]⁺ in the present study is discussed below. When more energetic CID conditions (higher collision energy and activation Q parameters associated with the ion trap instrument, see SI for details) were used, the homolytic cleavage of [U-CH₃]⁺ to make U⁺ and •CH₃ was observed (Figure S11.1 of the SI), providing evidence that the ion at m/z 253 that includes a U-CH₃ bond.

Subsequent isolation of $[U-CH_3]^+$ (Figure 1d) for reaction with background H_2O indicated that spontaneous hydrolysis occurs to create $[U(OH)]^+$ by reaction 2. The formation of the hydroxide product supports the assertion that reaction of $[UH]_+$ with acetonitrile creates $[U-CH_3]^+$. Formation of $[U(OH)]^+$ also provides evidence that spontaneous rearrangement of $[U-CH_3]^+$ to a structural isomer such as $[H-U=CH_2]^+$ by reaction 3 does not occur, as we expect the product ion in this case to be $[(OH)U=CH_2]^+$.

$$[U-CH_3]^+ + H_2O \rightarrow [U(OH)]^+ + CH_4$$
 (2)

$$[H-U=CH_2]^+ + H_2O \rightarrow [(OH)U=CH_2]^+ + H_2$$
 (3)

The next step was to change the neutral reagent to test for similar reactivity, and the experiments described above were performed with propionitrile (CH_3CH_2CN) as the neutral reagent. As shown in Figure 2a, isolation of [UH]⁺ to react with propionitrile led to the appearance of a peak at m/z 267, which is indicative of the production of [$U-CH_2CH_3$]⁺ by a reaction similar to 1.

Reaction of [UH]⁺ with Butyronitrile, Benzonitrile, and Acrylonitrile

To test the general approach to create a more extensive series of U-alkyls in the gas phase, experiments were continued using butyronitrile ($C_{\rm H_3}CH_2CH_2CN$), benzonitrile ($C_{\rm 6}H_{\rm 5}CN$), and acrylonitrile ($C_{\rm 2}H_{\rm 3}CN$) as neutral reagents. As shown in Figure 2, reactions with each neutral reagent created apparent U-alkyl species. For example, [UH]⁺ was found to react with butyronitrile ($CH_{\rm 3}CH_{\rm 2}CH_{\rm 2}CN$) to generate [U($CH_{\rm 2}CH_{\rm 2}CH_{\rm 3}$)]⁺ as indicated by the appearance of a peak at m/z 281. Reaction of [UH]⁺ with benzonitrile ($C_{\rm 6}H_{\rm 5}CN$) instead lead to formation of a peak at m/z 315, consistent with generation of a U-phenide,

 $[U(C_6H_5)]^+$ (Figure 3c). We next tested whether acrylonitrile could react by similar ion-molecule chemistry. As shown in Figure 3d, reaction of $[UH]^+$ with acrylonitrile (C_2H_3CN) lead to formation of a peak at m/z 265, consistent with the creation of the U-cation, $[U(C_2H_3)]^+$, formed by reaction 1.

Computational Investigation of Reaction Pathways

DFT calculations using the B3LYP⁵⁰ functional were employed to investigate the pathway by which the [U-R]⁺ species is formed by reactions of [UH]+ with nitriles. Complementary calculations were also performed using the PBE1PBE⁵¹ functional (included in the SI), which yielded qualitatively similar results. Potential minima, transition state structures, and their energies were identified using the reaction with [UH]⁺ and CH₃CN as the initial model system. Only the results for generation of [U-CH₃]⁺ are discussed in detail below for the sake of brevity. The pathways for reaction of [UH]⁺ with the other nitriles are qualitatively like those shown below for reaction with CH₃CN and the structures, energies, and reaction energy diagrams for generation of the other [U-R]⁺ species identified in the experiments are provided

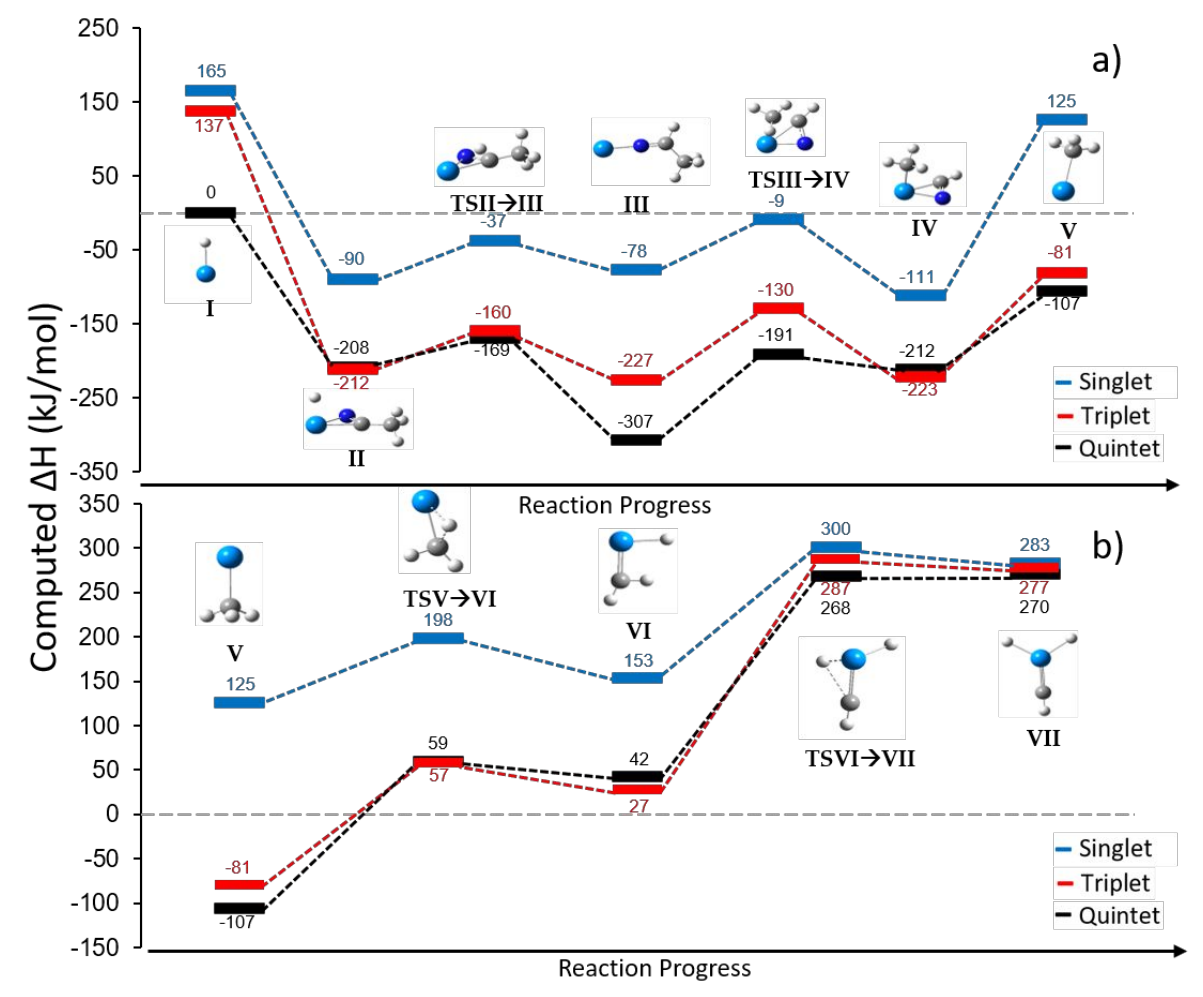


Figure 3: (a) Reaction energy diagram of $[UH]^+$ reacting with acetonitrile (CH_3CN) to create $[U-CH_3]^+$, calculated using B3LYP/SDD/6-311+g(d,p). (b) Reaction energy diagram of the rearrangement of $[U-CH_3]^+$. Singlet, triplet, and quintet spin surfaces are reported, coloured in blue, red, and black respectively. Enthalpies are relative to the reactants in the quintet spin state, which is the calculated ground state.

Journal Name ARTICLE

in the SI.

Figure 3a shows the calculated energy diagram for reaction of [UH]+ with acetonitrile. In general, the reaction is exothermic relative to the reactants (structure I) at 298.15K, which is consistent with the experimental observation that the reaction is spontaneous. Formation of the encounter complex (structure II) is predicted to be in a η -2 side-on coordination of the cyano (CN) group to U, with computed exothermicity of ca. 212 kJ/mol. An end-on U-N coordination of the nitrile was predicted to be higher in energy in all cases. Creation of intermediate III proceeds through transition state structure TSII \rightarrow III, which involves concerted breaking of side-on coordination of the CN group and transfer of hydride. Transfer of the methyl group to the uranium center to form an ion-molecule complex between [U-CH₃]+ and side-on coordinated HCN (intermediate IV) proceeds through TSIII \rightarrow IV.

Although the triplet spin state is predicted to be favored by approximately 10 kJ/mol, the energy difference between spin states is within the calculation's uncertainty. Furthermore, due to the near degeneracy of these spin states, the inclusion of spin-orbit coupling (or a fully relativistic calculation) would uniformly lower the energies of all species in the reaction pathway.53 Because the reaction energy diagram is primarily concerned with relative energy differences, this lowering would be similar across the intermediates and transition states, minimally affecting the key findings of the data. Additionally, while spin-orbit effects can be substantial for actinides, they are not directly relevant to testing the working hypothesis here. Their inclusion is important for producing highly accurate absolute thermochemical values, which are beyond the scope of this study and not experimentally verifiable in this context. Nevertheless, previous work by Armentrout and coworkers have shown that semi-empirical corrections for spin-orbit effects in actinides can provide valuable insights, and should be considered if applicable.57 The loss of HCN from the ionmolecule complex creates [U-CH₃]⁺ in the quintet spin state,

to acknowledge that DFT often overestimates the stability of high spin states, though this is unlikely to cause errors as large as 26 kJ/mol. Additionally, previous experimental and theoretical investigations into U complexes containing one σ -bonded ligand such as a hydride or a halogen have shown that the quintet spin is the ground state. $^{54-57}$

Assignment of Structure as σ-bonded [U-R]⁺ Species

Our experimental data suggests that reactions of [UH]+ with nitriles in the gas phase generates σ -bonded [U-R]⁺ products. Possible rearrangement of the σ -bonded U^{II}-methanide cation ([U-CH₃]⁺) to a structural isomer that, for example, contains a UVI center was investigated. This is shown by an extension of the reaction energy diagram (Figure 3b) and is relative to the energy of the initial reactants in the ground state (I). Here, the rearrangement of [U-CH₃]⁺ (V) occurs by transfer of a hydrogen from the σ -bound methanide to U to furnish the U^{IV} methylene hydride cation ($[U(H)(CH_2)]^+$) (VI) through TSV \rightarrow VI is predicted to be higher the initial reactants by ca. 57 kJ/mol. While rearrangement to form this isomer is possible, no evidence of this intermediate was provided by an investigation of reactions with H₂O discussed above: structures V and VI have the same m/z values but should display different reactivity (the latter should create the [UCH2OH]+ ion through and loss of H2). In addition, CID of [UCH₃]* confirmed that the connectivity is consistent with a sigma-bound complex due to the lack of $[UH_x]^+$ products. The reaction energy diagram for CID of [U-CH₃]⁺ is shown in the SI. Further rearrangement through the transfer of H from the methylene to U by TSVI→VII to create the possibly more thermodynamically stable UVI methylidyne dihydride ([U(H)₂(CH)]⁺) (VII) was determined to be improbable given the considerable kinetic barrier of ca. 270 kJ/mol in addition to this species being higher in energy than the σ -bonded complex (V). This indicates that the full rearrangement to a UVI species is unlikely.

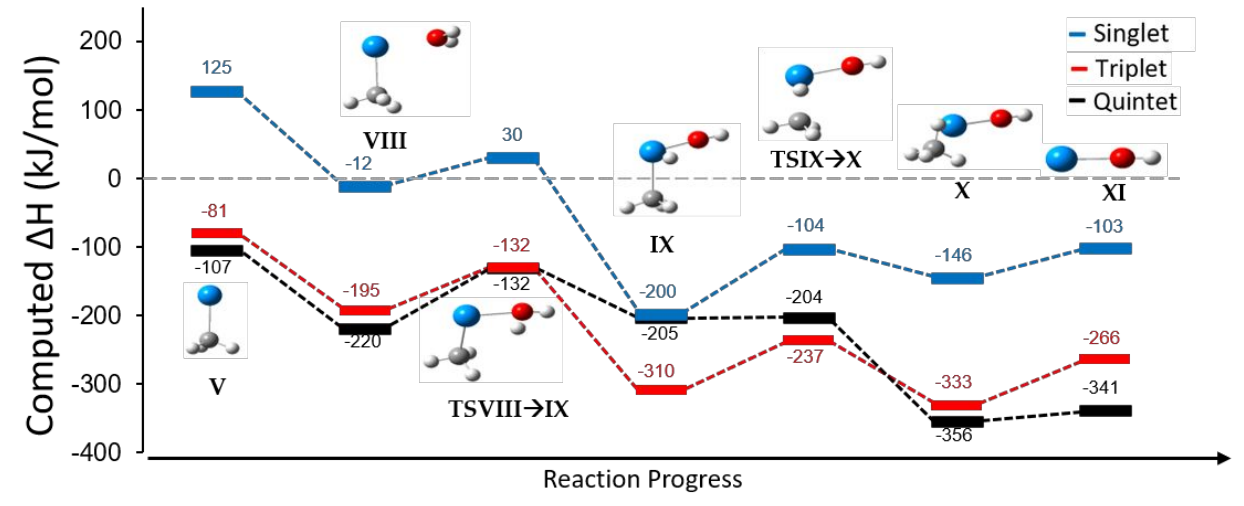


Figure 4: Reaction energy diagram of $[UCH_3]^+$ reacting with H_2O calculated using B3LYP/SDD/6-311+g(d,p). The enthalpies are relative to the ground state reactants ($[UH^+]$ and CH_3CN) as shown in Figure 3(a) given by B3LYP/SDD/6-311+g(d,p). Singlet, triplet, and quintet spin surfaces are reported, coloured in blue, red, and black respectively.

further supporting the $\sigma\text{-bonded U-R}$ structure. It is important

The CID reactions for the presumed [U-CH₃]⁺ species were also investigated using DFT. Specifically, the fragmentation processes leading to the formation of U+, [UCH2]+, and [UCH]+ were analyzed computationally. The reaction energy diagrams, found in the SI (Figures S10.1 and S10.2), reveal that the dissociation of [U-CH₃]⁺ to U⁺ and a methyl radical (•CH₃) is higher in energy than the rearrangement to the [H-U=CH₂]+ species by approximately 96 kJ/mol. However, the formation of $\ensuremath{\mathsf{U}^{\scriptscriptstyle{+}}}$ is energetically more favorable than the production of [UCH₂]⁺ by about 88 kJ/mol and [UCH]⁺ by about 44 kJ/mol. These findings are consistent with the calculated dissociation energy of the U⁺-CH₃ bond, which is approximately 262 kJ/mol, a value comparable to the previously reported U*-H bond dissociation energy of about 254 kJ/mol in our earlier study.⁴⁷ These results align reasonably well with the experimental work of Armentrout et al., which determined the U+-H bond dissociation energy to be 239.270 (±5.789) kJ/mol.⁵⁷ Based on this comparison, we can confidently predict that the bond dissociation energy of [UCH₃]⁺ follows a similar trend.

Moreover, the computational reaction energy diagrams show that the geometry of [U-CH₃]⁺ represents the global minimum. There is a spin state conversion from the quintet to the triplet when transitioning to the rearranged product, [H-U=CH₂]⁺ (VI). Interestingly, this rearrangement can be reversed with a small energy barrier of approximately 30 kJ/mol, indicating that the reverse reaction, from [H-U=CH₂]⁺ (VI) back to $[U-CH_3]^+$, is kinetically favorable. Consequently, $[U-CH_3]^+$ is likely the most abundant structural isomer present in the system. This conclusion aligns with observations by DiSanto et al., who found that the reaction of U+ with methane leads to a global minimum at the U-hydride methanide [H-U-CH₃]+ product, similar to what we report here.55 They also observed an endothermic rearrangement barrier to a U-methylidene at around 117 kJ/mol, which is comparable to our calculations, although applied to a slightly different system.⁵⁵

Hydrolysis of [U-CH₃]⁺ to create [UOH]⁺ and CH₄ was also investigated (Figure 4) to further support the claim of the σ bonded complex by the reactivity observed through experiment. To summarize, the hydrolysis of [U-CH₃]⁺ is predicted to be exothermic by ca. 234 kJ/mol and favors the quintet spin surface. The encounter complex (VIII) shows the exothermic coordination of water, which is ca. -114 kJ/mol relative to the initial reactants (I). The oxidative addition by H transfer from water to the metal to from the UIV-methanide hydride hydroxide complex (IX) is predicted to be bridged by the transition structure illustrated by structure TSVIII→IX. Oxidative addition from U^{II} to the U^{IV} species facilitates a spin transition to the triplet surface. Transfer of the hydride bound to uranium to the methanide ligand to form the $[UOH]^+$ CH_4 ionmolecule complex (X) is predicted by transition structure TSIX \rightarrow X, causing a spin transition back to the quintet surface.

Conclusions

To summarize, we have shown that the gas-phase ion-molecule reactions of [UH] $^+$ with a series of neutral nitriles lead to the formation of [U-R] $^+$ species (where R = CH₃, C₂H₅,

C₃H₇, or C₅H₆) along with hydrogen cyanide (HCN), as predicted by DFT calculations. This series of U-alkyls shows what is possible to be created in the gas-phase by PTMSⁿ, along with a facile way to create them for subsequent study of reactivity. The conclusion that σ-bonded species are formed is supported by DFT calculations that indicate a reaction pathway that involves hydride attack upon the nitrile C atom, and the elimination of neutral HCN. DFT calculations also suggest that spontaneous rearrangement of the formally U(II) alkyls to species with higher formal oxidation state such as [H2UCH]+ is not likely, strengthening the case that the unsupported, σbonded U(II) alkyl and aryl species are formed. Overall, the experimental and computational results align well and strongly suggest that the sigma-bound U-methanide structure is the dominant species. There is little evidence to support the existence of a U-hydride methylidene structure under the conditions of our study, further reinforcing our conclusion.

Future reactivity studies on these ions would be extremely helpful in the development of a theory for the reactivity of unsupported homoleptic U-alkyl complexes, along with the influences of f-electron involvement in chemistry. For example, from the observations of the series of experiments carried out, we hypothesize that there are other pathways to generate σ -bonded U-R species through reactions with [UH]⁺ and methane (CH₄), benzene (C₆H₆) by C-H activation and loss of H₂, or through a reaction with a carboxylic acid to generate a carboxylate ([U(CO₂-R)]) driven by the loss of H₂, and a subsequent collisional activation step to lose CO₂ and leave the U-R complex.

Author contributions

JT: investigation, methodology, writing – original draft, review, and editing. TAC: conceptualization, methodology, writing – review and editing. SL: investigation and methodology. MJV: conceptualization, methodology, writing – review and editing, project administration

Conflicts of interest

There are no conflicts of interest to declare.

Data availability

The data supporting this article have been included as part of the Supplementary Information.

Acknowledgements

J. G. T., T. A. C, and M. V. S. acknowledge support for this work from the School of Science and Engineering at Duquesne University. Laboratory space renovation partial support for this work by the National Science Foundation (CHE-0963450 and CHE-1950585) is also acknowledged. The Major Research

Journal Name ARTICLE

Instrumentation (MRI) Program CHE-1726824 is also gratefully acknowledged.

Notes and references

- S. A. Johnson and S. C. Bart, *Dalton Trans.*, 2015, 44, 7710–7726. https://doi.org/10.1039/c4dt01621a.
- H. Gilman, R. G. Jones, E. Bindschadler, D. Blume, G. Karmas,
 G. A. Martin, J. F. Nobis, J. R. Thirtle, H. L. Yale, and F. A. Yoeman, J. Am. Chem. Soc., 1956, 78, 2790–2792.
- 3 H. Gilman, Adv. Organomet. Chem., 1969, 7, 1–57.
- 4 A. R. Fox, S. C. Bart, K. Meyer, and C. C. Cummins, *Nature*, 2008, **455**, 341–349. https://doi.org/10.1038/nature07372.
- O. Ordoñez, X. Yu, G. Wu, J. Autschbach, and T. W. Hayton, *Inorg. Chem.*, 2021, 60, 12436–12444. https://doi.org/10.1021/acs.inorgchem.1c01686.
- 6 S. Fortier, B. C. Melot, G. Wu, and T. W. Hayton, *J. Am. Chem. Soc.*, 2009, **131**, 15512–15521. https://doi.org/10.1021/ja906516e.
- 7 T. J. Marks and A. M. Seyam, J. Am. Chem. Soc., 1972, 94, 6545–6546.
- 8 T. J. Marks, A. M. Seyam, and J. R. Kolb, *J. Am. Chem. Soc.*, 1973, **95**, 5529–5539.
- 9 E. R. Sigurdson and G. Wilkinson, J. Chem. Soc., Dalton Trans., 1977, 812–818.
- M. A. Boreen, B. F. Parker, T. D. Lohrey, and J. Arnold, J. Am. Chem. Soc., 2016, 138, 15865–15868. https://doi.org/10.1021/jacs.6b11182.
- 11 S. Fortier, J. L. Brown, N. Kaltsoyannis, G. Wu, and T. W. Hayton, *Inorg. Chem.*, 2012, **51**, 1625–1633. https://doi.org/10.1021/ic201936j.
- B. S. Newell, T. C. Schwaab, and M. P. Shores, *Inorg. Chem.*, 2011, 50, 12108–12115. https://doi.org/10.1021/ic201670z.
- 13 A. J. Wooles, M. Gregson, O. J. Cooper, A. Middleton-Gear, D. P. Mills, W. Lewis, A. J. Blake, and S. T. Liddle, *Organometallics*, 2011, 30, 5314–5325. https://doi.org/10.1021/om200553s.
- 14 S. J. Kraft, U. J. Williams, S. R. Daly, E. J. Schelter, S. A. Kozimor, K. S. Boland, J. M. Kikkawa, W. P. Forrest, C. N. Christensen, D. E. Schwarz, P. E. Fanwick, D. L. Clark, S. D. Conradson, and S. C. Bart, *Inorg. Chem.*, 2011, **50**, 9838–9848. https://doi.org/10.1021/ic2002805.
- 15 S. Fortier, J. R. Walensky, G. Wu, and T. W. Hayton, *J. Am. Chem. Soc.*, 2011, **133**, 11732–11743. https://doi.org/10.1021/ja204151v.
- 16 G. Ma, M. J. Ferguson, R. McDonald, and R. G. Cavell, *Inorg. Chem.*, 2011, **50**, 6500–6508. https://doi.org/10.1021/ic102537q.
- 17 J. L. Brown, C. C. Mokhtarzadeh, J. M. Lever, G. Wu, and T. W. Hayton, *Inorg. Chem.*, 2011, **50**, 5105–5112. https://doi.org/10.1021/ic200387n.
- 18 S. Fortier, J. R. Walensky, G. Wu, and T. W. Hayton, J. Am. Chem. Soc., 2011, 133, 6894–6897. https://doi.org/10.1021/ja2001133.
- 19 E. M. Matson, W. P. Forrest, P. E. Fanwick, and S. C. Bart, J. Am. Chem. Soc., 2011, 133, 4948–4954. https://doi.org/10.1021/ja110158s.
- 20 L. A. Seaman, S. Fortier, G. Wu, and T. W. Hayton, *Inorg. Chem.*, 2011, **50**, 636–646. https://doi.org/10.1021/ic101847b.
- 21 S. Fortier, G. Wu, and T. W. Hayton, *J. Am. Chem. Soc.*, 2010, **132**, 6888–6889. https://doi.org/10.1021/ja101567h.
- 22 F. MacGregor, A. Metta-Magaña, and S. Fortier, *Polyhedron*, 2024, 250, 116821. https://doi.org/10.1016/j.poly.2023.116821.
- 23 K. Li, J. He, Y. Zhao, and C. Zhu, *Inorg. Chem. Front.*, 2023, **10**, 5622–5633. https://doi.org/10.1039/D3QI01447A.

- 24 J. Shen, T. Rajeshkumar, G. Feng, Y. Zhao, S. Wang, L. Maron, and C. Zhu, *Angew. Chem.*, 2023, 135. https://doi.org/10.1002/ange.202303379.
- 25 J. Shen, T. Rajeshkumar, G. Feng, Y. Zhao, S. Wang, L. Maron, and C. Zhu, *Angew. Chem. Int. Ed.*, 2023, **62**. https://doi.org/10.1002/anie.202303379.
- 26 I. A. Popov, B. S. Billow, S. H. Carpenter, E. R. Batista, J. M. Boncella, A. M. Tondreau, and P. Yang, *Chem. Eur. J.*, 2022, 28. https://doi.org/10.1002/chem.202200114.
- 27 E. Lu, Actinide Metal Carbene Complexes: Synthesis, Structure and Reactivity, 2022, 312–346. https://doi.org/10.1016/B978-0-12-820206-7.00015-9.
- 28 T. W. Hayton, Hydride, Alkyl, Aryl, Acetylide, Carbonyl, and Cyanide Complexes of the Actinides, 2022, 58–84. https://doi.org/10.1016/B978-0-12-820206-7.00024-X.
- 29 A. J. Lewis, P. J. Carroll, and E. J. Schelter, J. Am. Chem. Soc., 2013, 135, 13185–13192. https://doi.org/10.1021/ja406610r.
- 30 J. H. Farnaby, T. Chowdhury, S. J. Horsewill, and B. Wilson, Buta- and Penta-Dienyl Complexes of the Actinides, 2022, 29– 81. https://doi.org/10.1016/B978-0-12-820206-7.00067-6.
- 31 S. L. Staun, G. Wu, W. W. Lukens, and T. W. Hayton, *Chem. Sci.*, 2021, **12**, 15519–15527. https://doi.org/10.1039/D1SC05072A.
- 32 G. T. Kent, X. Yu, G. Wu, J. Autschbach, and T. W. Hayton, Chem. Sci., 2021, 12, 14383–14388. https://doi.org/10.1039/D1SC04666G.
- 33 J. Murillo, R. Bhowmick, K. L. M. Harriman, et al., *Chem. Sci.*, 2021, 13360–13372. https://doi.org/10.1039/D1SC03275E.
- 34 S. Alvarez, *Eur. J. Inorg. Chem.*, 2021, **2021**, 3632–3647. https://doi.org/10.1002/ejic.202100500.
- 35 J. A. Seed, L. Birnoschi, E. Lu, et al., *Chem*, 2021, **7**, 1666–1680. https://doi.org/10.1016/j.chempr.2021.05.001.
- 36 S. T. Löffler and K. Meyer, *Actinides*, 2021, 471–521. https://doi.org/10.1016/B978-0-12-409547-2.14754-7.
- 37 J. D. Sears, D.-C. Sergentu, T. M. Baker, et al., Angew. Chem., 2020, 132, 13688–13692. https://doi.org/10.1002/ange.202005138.
- 38 M. J. Van Stipdonk, M. C. Michelini, A. Plaviak, et al., J. Phys. Chem. A, 2014, 118, 7838–7846. https://doi.org/10.1021/jp5066067.
- 39 Y. Gong, V. Vallet, M. C. Michelini, et al., *J. Phys. Chem. A*, 2014, **118**, 325–330. https://doi.org/10.1021/jp4113798.
- 40 Y. Gong, W. A. de Jong, and J. K. Gibson, J. Am. Chem. Soc., 2015, 137, 5911–5915. https://doi.org/10.1021/jacs.5b02420.
- 41 R. J. Abergel, W. A. de Jong, G. J.-P. Deblonde, et al., *Inorg. Chem.*, 2017, **56**, 12930–12937. https://doi.org/10.1021/acs.inorgchem.7b01720.
- S.-X. Hu, J. Jian, J. Li, and J. K. Gibson, *Inorg. Chem.*, 2019, 58, 10148–10159. https://doi.org/10.1021/acs.inorgchem.9b01265.
- 43 M. J. Van Stipdonk, I. J. Tatosian, A. C. Iacovino, et al., J. Am. Soc. Mass Spectrom., 2019, 30, 796–805. https://doi.org/10.1007/s13361-019-02179-6.
- 44 L. J. Metzler, C. T. Farmen, T. A. Corcovilos, and M. J. Van Stipdonk, *Phys. Chem. Chem. Phys.*, 2021, **23**, 4475–4479. https://doi.org/10.1039/D1CP00177A.
- 45 M. J. Van Stipdonk, E. H. Perez, L. J. Metzler, et al., *Phys. Chem. Chem. Phys.*, 2021, **23**, 11844–11851. https://doi.org/10.1039/D1CP01520F.
- 46 J. Terhorst, S. Lenze, L. Metzler, et al., *Dalton Trans.*, 2024, **53**, 5478–5483. https://doi.org/10.1039/d3dt02811a.
- 47 J. G. Terhorst, T. A. Corcovilos, and M. J. Van Stipdonk, J. Am. Soc. Mass Spectrom., 2023, 34, 2439–2442. https://doi.org/10.1021/jasms.3c00260.
- 48 E. Di Santo, M. C. Michelini, and N. Russo, *Organometallics*, 2009, 28, 3716–3726. https://doi.org/10.1021/om900156f.

- 49 R. M. Cox, A. D. French, K. M. Melby, et al., *The Energy Dependence of Transuranic Cation Reactions with Methane Observed by ICP-MS/MS*, Poster presented at the 72nd American Society for Mass Spectrometry Conference 2024. PNNL.
- 50 A. D. Becke, *J. Chem. Phys.*, 1993, **98**, 5648–5652. https://doi.org/10.1063/1.464913.
- 51 C. Adamo and V. Barone, *J. Chem. Phys.*, 1999, **110**, 6158–6170. https://doi.org/10.1063/1.478522.
- 52 I. O. Antonov and M. C. Heaven, *J. Phys. Chem. A*, 2013, **117**, 9684–9694. https://doi.org/10.1021/jp312362e.
- 53 P. Tufvesson, J. Lima-Ramos, M. Nordblad, and J. M. Woodley, WIREs Comput. Mol. Sci., 2011, 1, 760–780.
- 54 D. H. Bross and K. A. Peterson, *J. Chem. Phys.*, 2015, **143**, 184313. https://doi.org/10.1063/1.4935492.
- 55 E. Di Santo, M. C. Michelini, and N. Russo, J. Phys. Chem. A, 2009, 113, 14699–14705. https://doi.org/10.1021/jp9048154.
- 56 K. Balasubramanian, W. J. Siekhaus, and W. McLean, *J. Chem. Phys.*, 2003, **119**, 5889–5900. https://doi.org/10.1063/1.1601591.
- 57 W.-J. Zhang, M. Demireva, J. Kim, W. A. de Jong, and P. B. Armentrout, *J. Phys. Chem. A*, 2021, **125**, 7825–7839. https://doi.org/10.1021/acs.jpca.1c05409.

The data supporting this article is included in the main text or is included as part of the Supplementary Information.